Journal of Molecular Spectroscopy 310 (2015) 50–56

Contents lists available at ScienceDirect

Journal of Molecular Spectroscopy

journal homepage: www.elsevier.com/locate/jms

Infrared spectroscopic and theoretical study of the reactions of cerium atoms with methanol in solid argon

Yuzhen Li [a], Yu Gong [a], Xiaojie Zhou [a], Jing Su [b,c], Jun Li [b,*], Mingfei Zhou [a,*]

[a] Department of Chemistry, Shanghai Key Laboratory of Molecular Catalysts and Innovative Materials, Fudan University, Shanghai 200433, China
[b] Department of Chemistry & Key Laboratory of Organic Optoelectronics and Molecular Engineering of Ministry of Education, Tsinghua University, Beijing 100084, China
[c] Division of Nuclear Materials Science and Engineering, Shanghai Institute of Applied Physics and Key Laboratory of Nuclear Radiation and Nuclear Energy Technology, Chinese Academy of Sciences, Shanghai 201800, China

ARTICLE INFO

Article history:
Received 27 October 2014
In revised form 6 December 2014
Available online 18 December 2014

Keywords:
Methanol activation
Divalent cerium
Infrared spectroscopy
Matrix isolation
Reaction mechanism

ABSTRACT

Reactions of cerium metal atoms with methanol are investigated using matrix isolation infrared absorption spectroscopy and density functional theoretical calculations. Upon reaction of the ground state cerium metal atoms with methanol, the insertion intermediate CH_3OCeH is formed spontaneously on annealing in solid argon. Further sample annealing allows the reaction of CH_3OCeH with another methanol molecule to form H_2 and $Ce(OCH_3)_2$. The divalent $Ce(OCH_3)_2$ molecule can further isomerize to the more stable tetravalent $CH_3OCe(O)CH_3$ isomer under UV–visible irradiation. The product species are identified via isotopic substitutions and vibrational frequency calculations.

1. Introduction

Methanol has promising application in direct methanol fuel cells (DMFC) and is widely viewed as a renewable alternative to petroleum-based hydrocarbons. Of particular importance is the direct reforming of methanol into hydrogen [1]. As metals are often used as catalysts for the chemical transformation of methanol, it is vital to understand the interactions of methanol with metal centers at the molecular level [2]. A number of investigations on methanol reactions with main group, transition metal, and actinide metal atoms as well as metal oxide molecules have been carried out using matrix-isolation infrared spectroscopy [3–16], a powerful method for depicting reaction mechanisms through the isolation and characterization of reactive intermediates [17–20]. Both the O—H and C—O bond insertion molecules have been diagnosed as major reaction products. We recently found that reactions of early transition metals (Sc, Ti, V, Nb) with methanol led to facile formation of H_2 molecules [11]. This approach provides a simple and convenient pathway for producing hydrogen from methanol, a process that is of particular interest in fuel industry. Recent matrix isolation infrared spectroscopic investigations revealed that actinide (U) metal atoms could also react with two methanol molecules in solid argon to produce the divalent $U(OCH_3)_2$ product with one H_2 molecule released [12].

The reactions involving lanthanide metals exhibit unique trends across the whole lanthanide series because of the presence of 4f electrons [21–26]. Reactions between lanthanide cations from La^+ to Lu^+ (except Pm^+) and methanol molecules and clusters were studied in the gas phase using mass spectrometric methods. The majority of the lanthanide cations react exothermically with the methanol molecules, forming the dehydrogenation products. The study of the reaction sequences and of the corresponding kinetics showed the existence of important difference in the relative reactivity of the lanthanide series cations [27,28]. Recently, the reactions of late lanthanide metal atoms with methanol were studied using matrix isolation infrared spectroscopy [10]. It was shown that the reactions of Dy through Yb and methanol initially produced the $Ln(CH_3OH)$ complexes spontaneously upon annealing, which isomerized to the CH_3OLnH insertion products on visible light excitation. In addition, the Tb and Lu atoms could react with two methanol molecules to form the divalent $Ln(OCH_3)_2$ products spontaneously. In this paper, we report a combined matrix isolation infrared spectroscopic and theoretical investigation on the reaction of early lanthanide metal cerium atoms with methanol. Among the lanthanides, cerium is somewhat special because the easy conversion between trivalent and tetravalent Ce in chemistry. We will show that the reaction proceeds spontaneously on annealing to form the CH_3OCeH insertion intermediates, which can react further with another methanol molecule to give

* Corresponding authors.
E-mail addresses: junli@mail.tsinghua.edu.cn (J. Li), mfzhou@fudan.edu.cn (M. Zhou).

http://dx.doi.org/10.1016/j.jms.2014.12.013
0022-2852/

the dimethoxyl cerium molecule $Ce(OCH_3)_2$. This molecule can further isomerize to the more stable tetravalent Ce(IV) complex of $CH_3OCe(O)CH_3$ under photo-excitation. Theoretical studies show that these divalent Ce species has a triplet ground state with bent structure, while the tetravalent Ce species has a singlet state with a tetrahedral local coordination. The difference of tetravalent Ce and other trivalent lanthanides in reactivity towards methanol underscores the importance of oxidation states in heavy-element chemistry [29,30].

2. Experimental and theoretical methods

The cerium atoms were prepared by pulsed laser evaporation of bulk cerium metal targets. The experimental setup for pulsed laser evaporation and matrix isolation infrared spectroscopic investigation has been described in detail previously [31]. Briefly, the 1064 nm Nd:YAG laser fundamental (Continuum, Minilite II, 10 Hz repetition rate and 6 ns pulse width) was focused onto a freshly cleaned metal target (Johnson Matthey) through a hole in a CsI window cooled normally to 6 K by means of a closed-cycle helium refrigerator. Laser-evaporated metal atoms were co-deposited with methanol in excess argon onto the CsI window. The methanol/argon mixtures were prepared in a stainless steel vacuum line using standard manometric technique. Isotopically labeled $^{13}CH_3OH$ (Isotec, 99%), $CH_3^{18}OH$ (Isotec, 99%), CH_3OD (Isotec, 99%) and mixtures were used in different experiments. In general, matrix samples were deposited for 60 min at a rate of approximately 4 mmol/h. After sample deposition, infrared spectra of the resulting samples were recorded on a Bruker IFS 80 V spectrometer at a 0.5 cm^{-1} resolution between 4000 and 450 cm^{-1} using a liquid nitrogen cooled broad band HgCdTe (MCT) detector. Matrix samples were annealed to different temperatures and cooled back to 6 K for spectral acquisition. For selected samples, photoexcitations were performed through a quartz window mounted on the assembly. A 250 W high pressure mercury arc lamp ($250 < \lambda < 580$ nm) with different band pass filters (400 nm and 300 nm long-wavelength pass filters) was used.

Quantum chemical calculations were performed to determine the molecular structures and to help the assignments of vibrational frequencies of the observed reaction products. The calculations were performed at the level of density functional theory (DFT) with the hybrid B3LYP and BHandHLYP functionals [32–38]. The 6-311++G(d,p) basis sets were used for the H, C and O atoms, and the scalar-relativistic, energy-consistent effective-core potential (ECP) and corresponding SDD basis set was used for the Ce atom [39,40]. The 28 inert core electrons were included in the ECP, leaving the 4s, 4p, 4d, 5s, 5p, 5d, 6s and 4f electrons in the valence space for Ce. The SDD ECP and valence basis set were found to work well for similar reactions of Ln with CH_2F_2, CH_3F, CHF_3 and late lanthanide metal atoms with CH_3OH [10,41–43]. The geometries were fully optimized via analytic energy gradient algorithm. The stationary point was characterized as a minimum with all real vibrational frequencies or a transition state with one imaginary frequency in vibrational frequency calculations using analytic second derivatives of energy. The unscaled harmonic vibrational frequencies were used to determine the zero-point vibrational energies (ZPVE). To verify the reliability of the DFT energies, the single-point energies were calculated at the *ab initio* CCSD(T) level using the structures optimized at the BHandHLYP level with the same basis sets [44]. This mixed approach is abbreviated as CCSD(T)//BHandHLYP hereafter. Moreover, minimum energy paths (MEPs) were calculated by performing intrinsic reaction coordinates (IRC) analysis at the B3LYP and BHandHLYP levels of theory in both the forward and backward directions to confirm the transition states connecting the desired reactants and products [45]. All these calculations were performed using the Gaussian 09 program [46].

3. Results and discussion

3.1. Infrared spectra

The infrared spectra in selected regions from co-deposition of laser-evaporated Ce atoms with methanol molecules in excess argon are illustrated in Figs. 1 and 2, respectively. The product absorptions are listed in Table 1. The stepwise annealing and irradiation behaviors of the product absorptions are also shown in the figures and will be discussed below. The reaction between a cerium atom and methanol did not occur during deposition because of the very low concentration of methanol used (only 0.2%) and low evaporation laser energy. So no product absorptions were observed after sample deposition at 6 K except for the absorption due to CeO (808.4 cm^{-1}) in the low-frequency region [47]. New product absorptions were produced at 1287.4, 1269.5, 1263.1, 1135.5, 1114.2, 1113.0, 1111.8 and 1106.2 cm^{-1}, and the CeO absorption increased when the sample was annealed to 25 K (Figs. 1 and 2). The bands at 1135.5 and 1106.2 cm^{-1} increased, but other bands decreased slightly upon sample annealing to 35 K. When the sample was subjected to $250 < \lambda < 580$ nm broad band irradiation, the foregoing absorptions were completely destroyed, during which new absorptions at 1111.2 and 793.1 cm^{-1} were produced. These two bands increased upon further sample annealing.

Carbon-13, oxygen-18 and deuterium substitution experiments were performed for product identification through isotopic shift and splitting, and the isotopic counterparts are also listed in Table 1. Representative spectra in selected regions with different isotopic samples are shown in Figs. 3 and 4, respectively. All products gave isotopic doublets containing the same absorptions as in the pure isotopic experiments using the mixed isotopic samples except for the 1135.5 and 1106.2 cm^{-1} bands that produced triplets. The observation of triplet implies that these products require two methanol molecules as reactants.

3.2. Theoretical results

Geometry optimizations and frequency calculations were carried out on the stationary points in the reactions of Ce with methanol, including reactants, products, intermediates and transition states at the B3LYP and BHandHLYP levels of theory. The calculated vibrational frequencies of the species observed in our experiments are given in Table 2. The frequencies with isotopic substitutions are given in Table S1 of Supporting Information. The structural

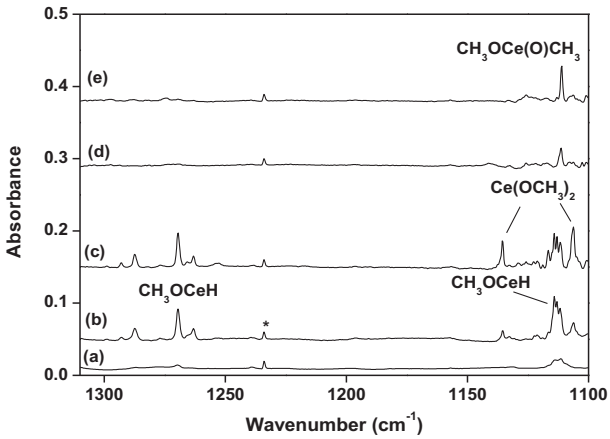

Fig. 1. Infrared spectra in the 1310–1100 cm^{-1} region from co-deposition of laser-evaporated cerium atoms with 0.2% CH_3OH in argon. (a) 1 h of sample deposition at 6 K, (b) after 25 K annealing, (c) after 35 K annealing, (d) after 15 min of $250 < \lambda < 580$ nm irradiation, and (e) after 30 K annealing (the asterisk denotes an unknown impurity absorption).

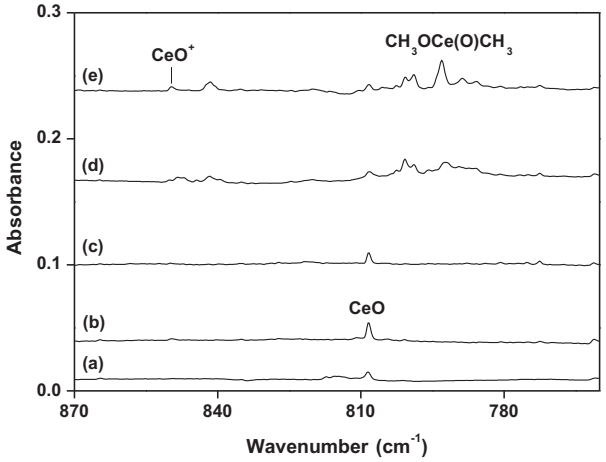

Fig. 2. Infrared spectra in the 870–760 cm^{-1} region from co-deposition of laser-evaporated cerium atoms with 0.15% CH_3OH in argon. (a) 1 h of sample deposition at 6 K, (b) after 25 K annealing, (c) after 35 K annealing, (d) after 15 min of 250 < λ < 580 nm irradiation, and (e) after 30 K annealing.

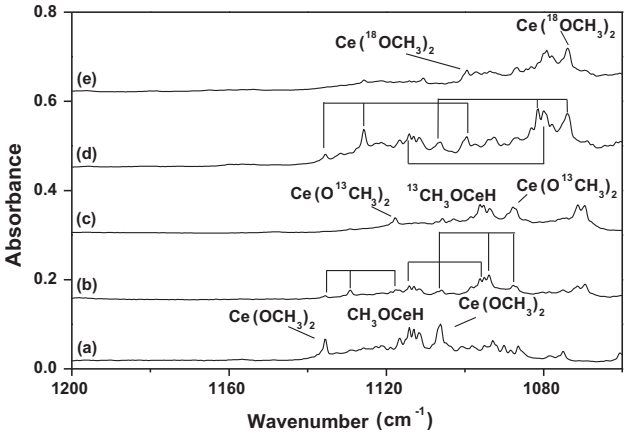

Fig. 3. Infrared spectra in the 1200–1060 cm^{-1} region from co-deposition of laser-evaporated cerium atoms with isotopic-labeled methanol in excess argon. Spectra were recorded after 1 h of sample deposition at 6 K followed by annealing at 35 K. (a) 0.15% CH_3OH, (b) 0.075% CH_3OH + 0.075% $^{13}CH_3OH$, (c) 0.15% $^{13}CH_3OH$, (d) 0.075% CH_3OH + 0.075% $CH_3^{18}OH$, and (e) 0.15% $CH_3^{18}OH$.

parameters of all stationary points are given in Fig. 5. The potential energy profile for the Ce and methanol reactions calculated at the BHandHLYP level of theory is shown in Fig. 6. Relative energies of the stationary points involved in the reactions calculated at the B3LYP, BHandHLYP and CCSD(T)//BHandHLYP levels are listed in Table S2 of Supporting Information.

For the Ce atom, the ground state has an electron configuration of $f^1d^1s^2$. The calculations predict that the $f^1_\alpha d^1_\alpha s^2$ triplet ground state is 3.1, 2.0 and 1.4 kcal/mol lower than the open-shell $f^1_\alpha d^1_\beta s^2$ singlet state at the B3LYP, BHandHLYP and CCSD(T)//BHandHLYP levels, respectively. Here the α and β indicate the up and down component of the electron spin. Since the singlet and triplet states of Ce are close in energy, we investigated the singlet- and triplet-state potential energy surfaces for the reaction of Ce atom and methanol. As expected, the energies at the potential energy surfaces of these two states are close to each other for all the stationary points with Ce(0) and Ce(II), but for $CH_3OCe(O)CH_3$ the triplet is much higher in energy because of its different electron configuration from the singlet ground state (Fig. 6 and Table S2). For some products, the vibrational frequencies calculated at the B3LYP level are slightly lower than the experimental results, but these frequencies at the BHandHLYP level are in good agreement with the experimental results (Tables 2 and S1). Therefore, the discussion is mainly based on the theoretical results from the BHandHLYP calculations.

3.3. CH_3OCeH

The 1269.5 and 1114.2 cm^{-1} absorptions produced simultaneously on 25 K annealing and decreased slightly on 35 K annealing. Both absorptions disappeared in concert on 250 < λ < 580 nm broad-band irradiation. These observations suggest that the two bands are probably due to different vibrational modes of the same molecule. The 1114.2 cm^{-1} absorption shifted to 1096.2 and 1080.0 cm^{-1}, respectively, in the experiments with the $^{13}CH_3OH$ and $CH_3^{18}OH$ samples. The $^{12}C/^{13}C$ and $^{16}O/^{18}O$ frequency ratios are 1.0164 and 1.0317, which are higher than the corresponding 1.0152 and 1.0254 ratios for methanol, but they

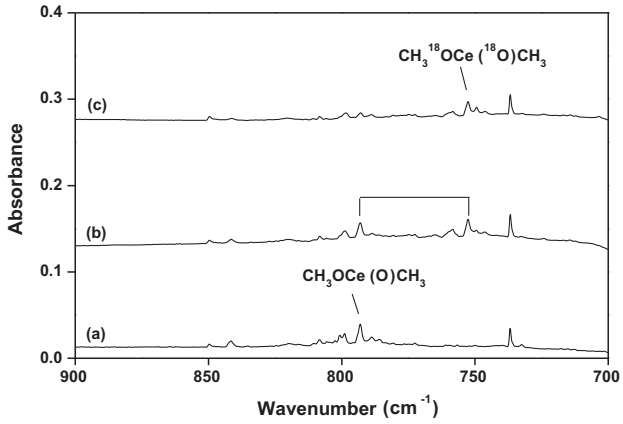

Fig. 4. Infrared spectra in the 900–700 cm^{-1} region from co-deposition of laser-evaporated cerium atoms with isotopic-labeled methanol in excess argon. Spectra were recorded after 1 h of sample deposition at 6 K and by 250 < λ < 580 nm irradiation followed by annealing to 30 K. (a) 0.15% CH_3OH, (b) 0.075% CH_3OH + 0.075% $CH_3^{18}OH$, and (c) 0.15% $CH_3^{18}OH$.

Table 1
Infrared absorptions (cm^{-1}) from the reactions of laser-evaporated Ce atoms with methanol in solid argon.

CH_3OH	$^{13}CH_3OH$	$CH_3^{18}OH$	$CH_3OH + {}^{13}CH_3OH$	$CH_3OH + CH_3^{18}OH$	CH_3OD	Assignment
1269.5	1269.3	1268.7	1269.4	1268.9	905.1	CH_3OCeH (Ce—H str.)
1287.4	1287.3	1286.6	1287.3	1287.0	917.9	Site
1263.1	1263.0	1262.3	1263.0	1262.7	900.5	Site
1114.2	1096.2	1080.0	1114.2, 1096.2	1114.2, 1080.0	1118.8	CH_3OCeH (C—O str.)
1113.0	1095.2	1079.2	1113.0, 1095.2	1113.0, 1079.2	1117.7	Site
1111.8	1093.7	1077.9	1111.8, 1093.7	1111.8, 1077.9	1116.3	Site
1135.5	1117.8	1099.5	1135.5, 1129.1, 1117.8	1135.5, 1125.6, 1099.5	1135.5	$Ce(OCH_3)_2$ (C—O sym. str.)
1106.2	1087.8	1073.7	1106.2, 1093.9, 1087.8	1106.2, 1081.4, 1073.7	1106.2	$Ce(OCH_3)_2$ (C—O asym. str.)
1111.2	1094.4	1073.9	1111.0, 1094.4	1111.2, 1073.9	1111.2	$CH_3OCe(O)CH_3$ (C—O str.)
793.1	792.8	752.6	792.8	792.8, 752.6	793.1	$CH_3OCe(O)CH_3$ (Ce=O str.)

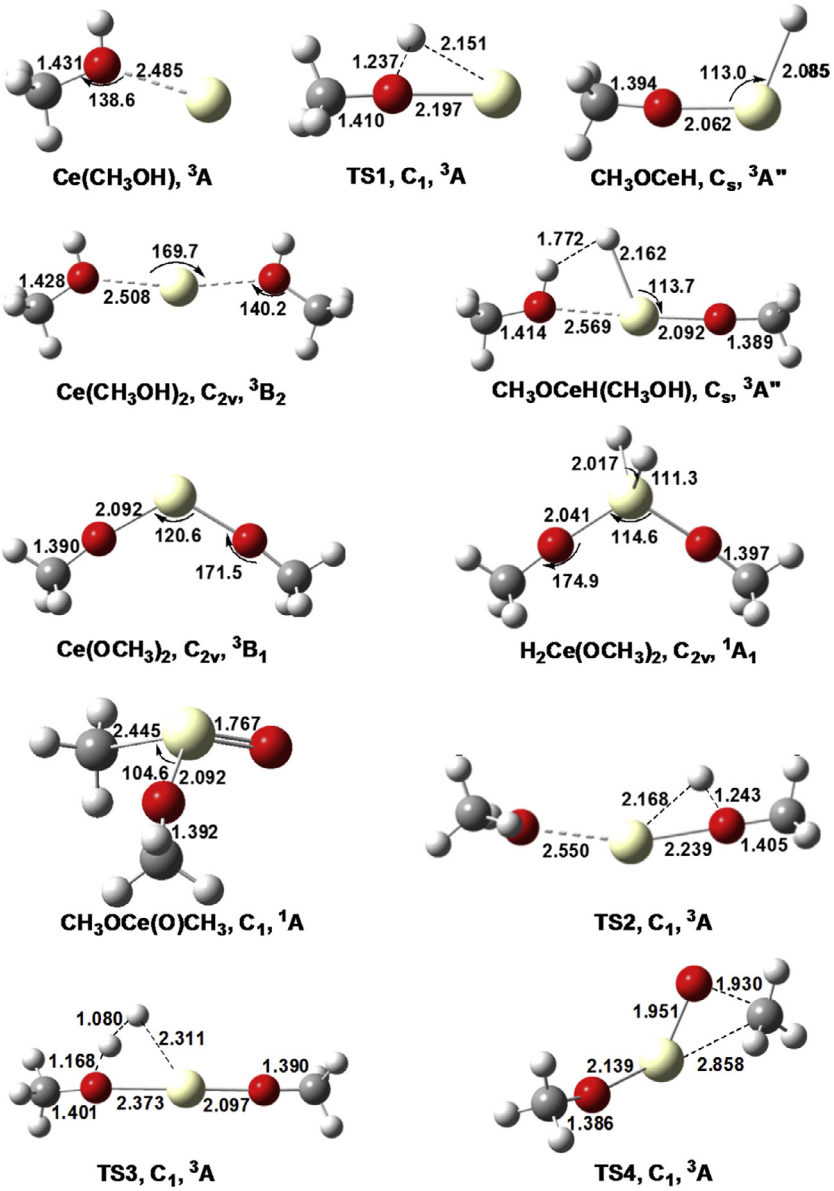

Fig. 5. Optimized geometries (bond lengths in angstrom, bond angles in degree) of the intermediates, transition states and products involved in the Ce + 2 CH_3OH reaction at the BHandHLYP level of theory.

bracket the characteristic ratios, 1.0225 and 1.0245, for the diatomic molecule C—O stretching vibration. The higher $^{16}O/^{18}O$ frequency ratio suggests that this mode has antisymmetric C—O stretching character. No intermediate absorption was observed in the mixed isotopic experiments (Fig. 3), indicating that only one CO moiety is involved in this mode. For the upper band at 1269.5 cm^{-1}, only small red shifts of 0.2 and 0.6 cm^{-1} were observed with the $^{13}CH_3OH$ and $CH_3^{18}OH$ samples, respectively. However, a large shift of 364.4 cm^{-1} to 905.1 cm^{-1} was found in the CH_3OD experiment with H/D frequency ratio of 1.4026 (Table 1). Hence the 1269.5 cm^{-1} absorption can be assigned to a Ce—H stretching vibration [48], which results from Ce insertion into the O—H bond of methanol. Note that the 1114.2 cm^{-1} band shifts higher to 1118.8 cm^{-1} in the deuterated sample, indicating interaction with a lower Ce—D mode. Hence CH_3OCeH is proposed here as the product molecule on the basis of the two experimentally observed infrared absorptions.

To verify the identification of the divalent CH_3OCeH molecule, DFT calculations were carried out to evaluate the energies and vibrational frequencies. The CH_3OCeH molecule was predicted by B3LYP and BHandHLYP calculations to have a $^3A''$ ground state with a Ce f^1s^1 electron subconfiguration with C_s symmetry (Fig. 5). The C—O bond length of this insertion product was calculated to be 1.394 Å at the BHandHLYP level (1.409 Å at the B3LYP level), in the region of typical C—O single bonds [8–10]. The C—O and Ce—H stretching vibrational frequencies were calculated at 1186.0 and 1368.4 cm^{-1} with the strongest intensities at the BHandHLYP level (Table 2). These frequencies lie at 1116.2 and 1330.2 cm^{-1} at the B3LYP level (see Table S1). The theoretical H/D, $^{12}C/^{13}C$ and $^{16}O/^{18}O$ ratios are in good agreement with the experimental results (Table 2).

3.4. $Ce(OCH_3)_2$

Two absorptions at 1135.5 and 1106.2 cm^{-1} were produced upon annealing to 25 K, which increased on annealing to 35 K during which the intensity of the CH_3OCeH absorptions decreased slightly. When the sample was subjected to $250 < \lambda < 580$ nm broad band irradiation, these two absorptions disappeared. The 1135.5 and 1106.2 cm^{-1} absorptions shift to 1117.8 and

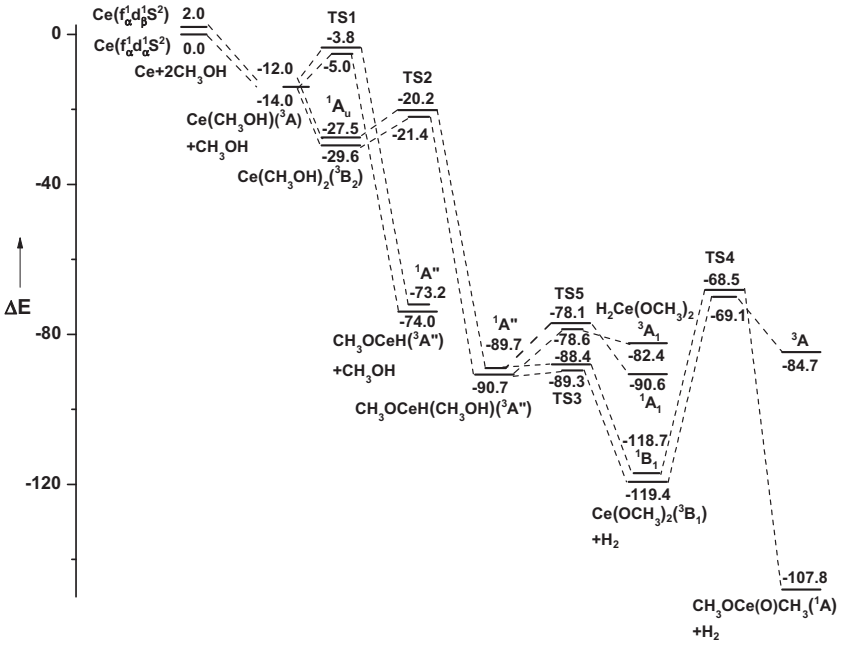

Fig. 6. The triplet and singlet potential energy profiles of the Ce + 2 CH_3OH reaction calculated at the BHandHLYP level of theory. The energies (kcal/mol) are corrected with zero-point vibrational energies.

Table 2
Comparison between the observed and calculated (BHandHLYP) vibrational frequencies (cm^{-1}) and isotopic frequency ratios of the products.

Mode	Freq		$^{12}C/^{13}C$		$^{16}O/^{18}O$		H/D[a]	
	Obsd[b]	Calcd[c]	Obsd	Calcd	Obsd	Calcd	Obsd	Calcd
CH_3OCeH, C_s, $^3A''$								
Ce—H str.	1269.5(1.00)	1368.4(696)	1.0002	1.0021	1.0006	1.0028	1.4026	1.4177
C—O str.	1114.2(0.64)	1186.0(605)	1.0164	1.0152	1.0317	1.0311	0.9959	0.9940
$Ce(OCH_3)_2$, C_{2v}, $^3B_1$								
C—O sym. str.	1135.5(0.84)	1209.3(302)	1.0158	1.0143	1.0327	1.0320	1.0000	1.0000
C—O asym. str.	1106.2(1.00)	1178.5(664)	1.0169	1.0166	1.0303	1.0303	1.0000	1.0000
$CH_3OCe(O)CH_3$, C_1, ^1A								
C—O str.	1111.2(1.00)	1184.5(422)	1.0154	1.0161	1.0347	1.0313	1.0000	1.0000
Ce=O str.	793.1(0.72)	882.7(401)	1.0004	0.9964	1.0538	1.0495	1.0000	1.0000

[a] D refers to CH_3OD reaction product.
[b] Integrated intensity normalized to the most intense absorption.
[c] Calculated IR intensity in km/mol.

1087.8 cm^{-1} with $^{13}CH_3OH$, exhibiting the $^{12}C/^{13}C$ isotopic frequency ratios of 1.0158 and 1.0169, respectively. Upon $^{16}O/^{18}O$ substitution, these two absorptions shift to 1099.5 and 1073.7 cm^{-1} with the $^{16}O/^{18}O$ isotopic frequency ratios of 1.0327 and 1.0303. The band position and isotopic frequency ratios revealed that the 1135.5 and 1106.2 cm^{-1} absorptions are due to C—O stretching vibration modes. In the mixed $CH_3OH + {}^{13}CH_3OH$ experiment, two triplets were observed with intermediate absorptions at 1129.1 and 1093.9 cm^{-1} (Fig. 3), and two triplets with intermediate absorptions at 1125.6 and 1081.4 cm^{-1} were also observed in the mixed $CH_3OH + CH_3^{18}OH$ experiment, indicating the existence of two equivalent C—O moieties in this new molecule. Since no other absorption was found, we assign the two bands at 1135.5 and 1106.2 cm^{-1} to the symmetric and antisymmetric C—O stretching vibrations of the $Ce(OCH_3)_2$ molecule.

Our DFT calculations predict that the $Ce(OCH_3)_2$ molecule to have a $^3B_1$ ground state with a Ce f^1s^1 electron subconfiguration (Fig. 5). The Ce—O bond length is 2.092 Å, slightly longer than that of CH_3OCeH. As listed in Table S3, the infrared absorptions predicted at 1209.3 and 1178.5 cm^{-1} for symmetric and antisymmetric C—O stretching modes are much stronger than the others. These calculated frequencies correlate well with the observed 1135.5 and 1106.2 cm^{-1} frequency. The good correlation between the experimental and theoretical isotopic ratios further support the assignment of the $Ce(OCH_3)_2$ molecule (Table 2). Similar to the $M(OCH_3)_2$ (M = Tb, Lu, U) molecules identified previously [10,12], the $Ce(OCH_3)_2$ molecule also has a bent geometry with the OCeO bond angle of 120.6°, which is different from the vanadium and titanium analogues that feature linear structures [11]. This geometry difference of dimethoxyl complexes of early transition metals and Ce is likely due to interaction between d-orbitals and the lone-pairs on the CH_3O ligand.

3.5. $CH_3OCe(O)CH_3$

The 1111.2 and 793.1 cm^{-1} absorptions were produced on irradiation at the expense of the $Ce(OCH_3)_2$ absorptions, suggesting that this new product is probably a structural isomer of the $Ce(OCH_3)_2$ molecule. Isotopic substitution revealed that the $^{12}C/^{13}C$ and $^{16}O/^{18}O$ frequency ratios for the 1111.2 cm^{-1} absorp-

tion were 1.0154 and 1.0347, respectively, similar to those for the C—O stretching vibration in CH_3OCeH. The 793.1 cm^{-1} band shifted to 752.6 cm^{-1} when cerium atoms reacted with $CH_3^{18}OH$, but it only slightly shifted 0.3 cm^{-1} in the experiment with $^{13}CH_3OH$ (Fig. 4). This 40.5 cm^{-1} red shift from the frequency with $CH_3^{18}OH$ defines the $^{16}O/^{18}O$ ratio as 1.0538, which is about the same as isotopic ratio for the diatomic CeO molecule (1.0537) and is characteristic of a Ce=O stretching vibration [47]. The doublet isotopic structures in the experiment with equal molar mixtures of CH_3OH and $CH_3^{18}OH$ confirmed the involvement of only one Ce=O subunit (Fig. 4). On the basis of observation of the 1111.2 and 793.1 cm^{-1} absorptions, the new molecule should involve a $CH_3OCe(O)$ moiety, and its formation requires two methanol molecules. Similar to the $CH_3OU(O)CH_3$ molecule identified in the reaction of uranium and methanol [12], the $CH_3OCe(O)CH_3$ structure with one methoxyl group and one methyl group attached to the cerium center of CeO is proposed for the candidate molecule, which absorbs at 1111.2 and 793.1 cm^{-1}.

The $CH_3OCe(O)CH_3$ molecule was predicted by DFT calculations to have a singlet ground state with a pyramidal geometry and a Ce(IV) center. The two strongest infrared absorptions due to Ce=O and C—O stretching modes were calculated at 882.7 and 1184.5 cm^{-1}. The $^{12}C/^{13}C$ and $^{16}O/^{18}O$ frequency ratios of these two bands predicted from isotopic calculations are in good agreement with the experimental values (Table 2).

3.6. Reaction mechanisms

The reaction of cerium metal atom with methanol in solid argon can be proposed as the following on the basis of the experimental observations (Scheme 1).

Similar to the reactions of scandium, uranium, terbium and lutetium atoms with methanol molecules [9–12], the inserted CH_3OCeH product was formed spontaneously during sample annealing without the observation of the $Ce(CH_3OH)$ complex. In the reactions of late lanthanide metal atoms, the inserted CH_3OLnH molecules were produced under visible light irradiation via the $Ln(CH_3OH)$ complex intermediates. The absence of the $Ce(CH_3OH)$ complex is probably due to the low insertion reaction barriers to form the CH_3OCeH molecule. The potential energy profiles shown in Fig. 6 suggest that the formation of the $Ce(CH_3OH)$ complex from Ce atom and CH_3OH is spontaneous. The exothermicity (14.0 kcal/mol) of this complex formation is sufficient to provide energy to get over the 9.0 kcal/mol barrier from $Ce(CH_3OH)$ to CH_3OCeH (TS1), which lies below the Ce + CH_3OH reactants by 5.0 kcal/mol. It is conceivable that the C—O insertion reaction to produce CH_3OCeH is spontaneous, as observed experimentally. This also suggests that the $Ce(CH_3OH)$ complex is very short-lived, rapidly rearranging to form the CH_3OCeH molecule on annealing.

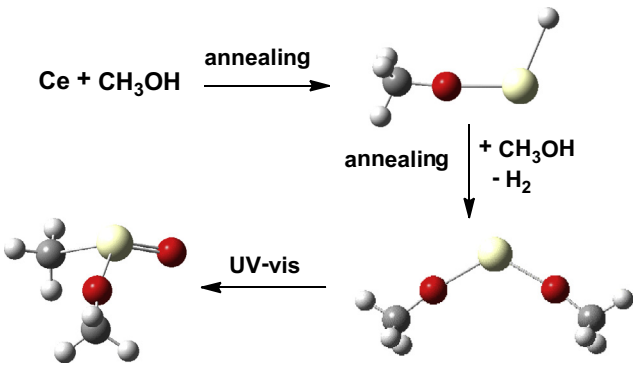

Scheme 1.

The initially formed CH_3OCeH molecule can subsequently react with another methanol molecule to give the respective $Ce(OCH_3)_2$ molecule with H_2 elimination. The reaction was predicted to proceed with the formation of a $CH_3OCeH(CH_3OH)$ intermediate via a transition state (TS2) lying 5.8 kcal/mol above the $Ce(CH_3OH)_2$ complex at the CCSD(T) level. This barrier is slightly lower than that of the formation of CH_3OCeH. The $CH_3OCeH(CH_3OH)$ complex with the O—Ce—O bond angle close to 180.0° is 92.1 kcal/mol lower than the reactants Ce + 2 CH_3OH. The $CH_3OCeH(CH_3OH)$ complex allows the formation of an intermolecular H···H bond between the hydridic H bonded to Ce and the protic H on the O. The H···H bond distance is only 1.772 Å in $CH_3OCeH(CH_3OH)$. From the $CH_3OCeH(CH_3OH)$ intermediate, the reaction proceeds to the $Ce(OCH_3)_2 + H_2$ products via a transition state (TS3) with a negligible barrier (1.4 kcal/mol) and an exothermicity of 28.7 kcal/mol. The transition state TS3 has a geometry qualitatively like that of the $CH_3OCeH(CH_3OH)$ complex; the main differences are the decrease of the H H and O(H)—Ce bond lengths. The overall reaction from Ce + 2 CH_3OH to $Ce(OCH_3)_2 + H_2$ was predicted to be exothermic by 122.1 kcal/mol at the CCSD(T) level, and proceeds via two transition states lying lower in energy (21.4 and 89.3 kcal/mol at the BHandHLYP level) than the reactants. Hence, the overall reaction is both thermodynamically favorable and spontaneous in each kinetic step.

The $Ce(OCH_3)_2$ molecule can further isomerize to the more stable cerium (IV) $CH_3OCe(O)CH_3$ product on UV–visible irradiation, which is similar to the reaction mechanism of methanol with uranium [12]. Filtered experiment with high pressure mercury arc lamp indicates that only the light in the wavelength range of 250–300 nm is responsible for the observed photochemistry. The cerium (IV) $CH_3OCe(O)CH_3$ molecule is 26.0 kcal/mol lower in energy than the cerium (II) $Ce(OCH_3)_2$ isomer at the CCSD(T) level. The $Ce(OCH_3)_2$ molecule has a triplet ground state, whereas the $CH_3OCe(O)CH_3$ isomer has a singlet ground state. Thus, the crossing of adiabatic surfaces of different spin is involved in the isomerization reaction. Previous studies have shown that transition-metal-mediated reactions very often occur on more than one adiabatic potential energy surfaces [49,50]. Calculations predict that the isomerization reaction proceeds via a transition state (TS4) lying about 50 kcal/mol above $Ce(OCH_3)_2$ on both singlet and triplet energy surfaces at the BHandHLYP level, consistent with the experimental observation that the isomerization reaction is a photochemical process.

In contrast to $Ce(OCH_3)_2$, the $Ln(OCH_3)_2$ molecules of late lanthanide metals cannot isomerize to the $CH_3OLn(O)CH_3$ isomers under UV–visible excitation. Such difference is likely due to the stable oxidation state of IV for Ce and III or II for the late lanthanides.

4. Conclusions

The reaction of cerium metal atom with methanol molecules has been investigated using matrix isolation infrared spectroscopy and quantum chemistry. The experiments show that the CH_3OCeH and $Ce(OCH_3)_2$ molecules can be produced spontaneously on annealing. This result indicates that dihydrogen can be produced directly from the reaction of ground-state cerium metal atoms with methanol even at cryogenic temperatures as found previously for terbium, lutetium, uranium and early transition metal atoms. The observation of these spontaneous reactions are consistent with theoretical predictions that both the reactions Ce + $CH_3OH \rightarrow CH_3OCeH$ and Ce + 2 $CH_3OH \rightarrow Ce(OCH_3)_2 + H_2$ are thermodynamically exothermic and each elementary reaction steps are kinetically facile, requiring little activation energy. The divalent $Ce(OCH_3)_2$ molecule further rearranges to the tetravalent $CH_3OCe(O)CH_3$ isomer

with $250 < \lambda < 580$ nm irradiation. The $CH_3OCe(O)CH_3$ molecule is predicted to have a singlet ground state with pyramidal structure.

Acknowledgments

This work was supported by the Ministry of Science and Technology of China (2013CB834603), the National Natural Science Foundation of China (Grant Nos. 21173053, 21433005 and 91026003) and the Committee of Science and Technology of Shanghai (13XD1400800). The calculations were performed at the Tsinghua National Laboratory for Information Science and Technology, and Shanghai Supercomputing Center.

Appendix A. Supplementary material

Supplementary data for this article are available on ScienceDirect (www.sciencedirect.com) and as part of the Ohio State University Molecular Spectroscopy Archives (http://library.osu.edu/sites/msa/jmsa_hp.htm). Also follow style instructions from previous Word version of style sheet. Supplementary data associated with this article can be found, in the online version, at http://dx.doi.org/10.1016/j.jms.2014.12.013.

References

[1] G.A. Olah, Angew. Chem. Int. Ed. 44 (2005) 2636–2639, http://dx.doi.org/10.1002/anie.200462121.
[2] J. Greeley, M. Mavrikakis, J. Am. Chem. Soc. 126 (2004) 3910–3919, http://dx.doi.org/10.1021/ja037700z.
[3] M. Park, R.H. Hauge, Z.H. Kafafi, J.L. Margrave, J. Chem. Soc. Chem. Commun. 22 (1985) 1570–1571, http://dx.doi.org/10.1039/c39850001570.
[4] V.N. Khabashesku, K.N. Kudin, J.L. Margrave, L. Fredin, J. Organomet. Chem. 595 (2000) 248–260, http://dx.doi.org/10.1016/S0022-328X(99)00632-4.
[5] Z.G. Huang, M.H. Chen, Q.N. Liu, M.F. Zhou, J. Phys. Chem. A 107 (2003) 11380–11385, http://dx.doi.org/10.1021/jp035652z.
[6] H.A. Joly, J.A. Howard, G.A. Arteca, Phys. Chem. Chem. Phys. 3 (2001) 750–759, http://dx.doi.org/10.1039/b007650n.
[7] D.V. Lanzisera, L. Andrews, J. Phys. Chem. A 101 (1997) 1482–1487, http://dx.doi.org/10.1021/jp963749y.
[8] Z.G. Huang, M.H. Chen, M.F. Zhou, J. Phys. Chem. A 108 (2004) 3390–3395, http://dx.doi.org/10.1021/jp038028v.
[9] M.H. Chen, Z.G. Huang, M.F. Zhou, J. Phys. Chem. A 108 (2004) 5950–5955, http://dx.doi.org/10.1021/jp048348u.
[10] Y. Gong, L. Andrews, M.Y. Chen, D.A. Dixon, J. Phys. Chem. A 115 (2011) 14581–14592, http://dx.doi.org/10.1021/jp209135a.
[11] G.J. Wang, J. Su, Y. Gong, M.F. Zhou, J. Li, Angew. Chem. Int. Ed. 49 (2010) 1302–1305, http://dx.doi.org/10.1002/anie.200906473.
[12] Y. Gong, L. Andrews, Inorg. Chem. 50 (2011) 7099–7105, http://dx.doi.org/10.1021/ic200618x.
[13] B.S. Ault, J. Am. Chem. Soc. 120 (1998) 6105–6112, http://dx.doi.org/10.1021/ja9808752.
[14] E.M. Schierloh, B.S. Ault, J. Phys. Chem. A 107 (2003) 2629–2634, http://dx.doi.org/10.1021/jp022427t.
[15] B.S. Ault, J. Phys. Chem. A 103 (1999) 11474–11480, http://dx.doi.org/10.1021/jp993318q.
[16] G.J. Wang, J. Zhuang, M.F. Zhou, J. Phys. Chem. A 115 (2011) 8623–8629, http://dx.doi.org/10.1021/jp204359a.
[17] V.E. Bondybey, A.M. Smith, J. Agreiter, Chem. Rev. 96 (1996) 2113–2134, http://dx.doi.org/10.1021/cr940262h.
[18] H.J. Himmel, A.J. Downs, T.M. Greene, Chem. Rev. 102 (2002) 4191–4242, http://dx.doi.org/10.1021/cr020405x.
[19] M.F. Zhou, L. Andrews, C.W. Bauschlicher Jr., Chem. Rev. 101 (2001) 1931–1961, http://dx.doi.org/10.1021/cr990102b.
[20] Y. Gong, M.F. Zhou, L. Andrews, Chem. Rev. 109 (2009) 6765–6808, http://dx.doi.org/10.1021/cr900185x.
[21] J. Xu, X. Jin, M.F. Zhou, J. Phys. Chem. A 111 (2007) 7105–7111, http://dx.doi.org/10.1021/jp073047g.
[22] J. Xu, M.F. Zhou, J. Phys. Chem. A 110 (2006) 10575–10582, http://dx.doi.org/10.1021/jp063776g.
[23] W.H. Xu, X. Jin, M.H. Chen, P. Pyykko, M.F. Zhou, J. Li, Chem. Sci. 3 (2012) 1548–1554, http://dx.doi.org/10.1039/c2sc00998f.
[24] K. Hong, J. Kim, T.K. Kim, Bull. Korean, Chem. Soc. 34 (2013) 1551–1554, http://dx.doi.org/10.5012/bkcs.2013.34.5.1551.
[25] P. Cheng, G.K. Koyanagi, D.K. Bohme, Chem. Phys. Chem. 7 (2006) 1813–1819, http://dx.doi.org/10.1002/cphc.200600248.
[26] G.K. Koyanagi, P. Cheng, D.K. Bohme, J. Phys. Chem. A 114 (2010) 241–246, http://dx.doi.org/10.1021/jp9079487.
[27] W.Y. Lu, S.H. Yang, J. Phys. Chem. A 102 (1998) 1954–1962. http://dx.doi.org/10.1021/jp980151c.
[28] J.M. Carretas, J. Marcalo, A.P. de Matos, Int. J. Mass Spectrom. 234 (2004) 51–61, http://dx.doi.org/10.1016/j.ijms.2004.01.018.
[29] G.J. Wang, M.F. Zhou, J.T. Goettel, G.J. Schrobilgen, J. Su, J. Li, T. Schloeder, S. Riedel, Nature 514 (2014) 475–477, http://dx.doi.org/10.1038/nature13795.
[30] W. Huang, W.H. Xu, J. Su, W.H.E. Schwarz, J. Li, Inorg. Chem. 52 (2013) 14237–14245, http://dx.doi.org/10.1021/ic402170q.
[31] G.J. Wang, M.F. Zhou, Int. Rev. Phys. Chem. 27 (2008) 1–25, http://dx.doi.org/10.1080/01442350701685946.
[32] P. Hohenberg, W. Kohn, Phys. Rev. 136 (1964) B864–B871, http://dx.doi.org/10.1103/PhysRev.136.B864.
[33] W. Kohn, L.J. Sham, Phys. Rev. 140 (1965) A1133–A1138, http://dx.doi.org/10.1103/PhysRev.140.A1133.
[34] R.G. Parr, W. Yang, Density-Functional Theory of Atoms and Molecules, Oxford Univ. Press, Oxford, U.K., 1989.
[35] D.R. Salahub, M.C. Zerner (Eds.), The Challenge of d and f Electrons, American Chemical Society, Washington, D.C., 1989.
[36] A.D. Becke, J. Chem. Phys. 98 (1993) 5648–5652, http://dx.doi.org/10.1063/1.464913.
[37] C. Lee, W. Yang, R.G. Parr, Phys. Rev. B 37 (1988) 785–789, http://dx.doi.org/10.1103/PhysRevB.37.785.
[38] A.D. Becke, J. Chem. Phys. 98 (1993) 1372–1377, http://dx.doi.org/10.1063/1.464304.
[39] M. Dolg, H. Stoll, H. Preuss, J. Chem. Phys. 90 (1989) 1730–1734, http://dx.doi.org/10.1063/1.456066.
[40] X. Cao, M. Dolg, J. Mol. Struct. (THEOCHEM) 581 (2002) 139–147, http://dx.doi.org/10.1016/S0166-1280(01)00751-5.
[41] X.F. Wang, H.G. Cho, L. Andrews, M.Y. Chen, D.A. Dixon, H.S. Hu, J. Li, J. Phys. Chem. A 115 (2011) 1913–1921, http://dx.doi.org/10.1021/jp111592e.
[42] M.Y. Chen, D.A. Dixon, X.F. Wang, H.G. Cho, L. Andrews, J. Phys. Chem. A 115 (2011) 5609–5624, http://dx.doi.org/10.1021/jp2009572.
[43] Y. Gong, X. Wang, L. Andrews, M.Y. Chen, D.A. Dixon, Organometallics 30 (2011) 4443–4452, http://dx.doi.org/10.1021/om200533q.
[44] A.J. Pople, M. Head-Gordon, K. Raghavachari, J. Chem. Phys. 87 (1987) 5968–5975, http://dx.doi.org/10.1063/1.453520.
[45] C. Gonzalez, H.B. Schlegel, J. Chem. Phys. 90 (1989) 2154–2161, http://dx.doi.org/10.1063/1.456010.
[46] M.J. Frisch, G.W. Trucks, H.B. Schlegel, G.E. Scuseria, M.A. Robb, J.R. Cheeseman, G. Scalmani, V. Barone, B. Mennucci, G.A. Petersson, et al., Gaussian 09, Revision B.01, Gaussian Inc., Wallingford, CT, 2009.
[47] S.P. Willson, L. Andrews, J. Phys. Chem. A 103 (1999) 3171–3183, http://dx.doi.org/10.1021/jp990005m.
[48] S.P. Willson, L. Andrews, J. Phys. Chem. A 104 (2000) 1640–1647, http://dx.doi.org/10.1021/jp993038a.
[49] N. Russo, E. Sicilia, J. Am. Chem. Soc. 123 (2001) 2588–2596, http://dx.doi.org/10.1021/ja000658c.
[50] S.P. de Visser, F. Ogliaro, N. Harris, S. Shaik, J. Am. Chem. Soc. 123 (2001) 3037–3047, http://dx.doi.org/10.1021/ja003544+.